Cellular Physiology and Biochemistry

Cell Physiol Biochem 2018;50:2296-2313
DOI: 10.1159/000495089
Published online: 13 November 2018
Accepted: 5 November 2018

Original Paper

Ca^{2+} Signaling Triggered by Shear-Autocrine P2X Receptor Pathway in Rat Atrial Myocytes

Joon-Chul Kim Min-Jeong Son Sun-Hee Woo

Laboratory of Physiology, College of Pharmacy, Chungnam National University, Daejeon, South Korea

Key Words
Shear stress • AP-triggered Ca^{2+} wave • Atrial myocytes • ATP release • P2X recceptor

Abstract
Background/Aims: The atrium is exposed to high shear stress during heart failure and valvular diseases. We aimed to understand atrial shear-induced Ca^{2+} signaling and its underlying mechanisms. ***Methods:*** Pressurized micro-flow was applied to single rat atrial myocytes, and Ca^{2+} signal, membrane potential, and ATP release were assessed using confocal imaging, patch clamp technique, and luciferin-luciferase assay, respectively. ***Results:*** Shear stress (~16 dyn/cm^2) induced global Ca^{2+} waves (~0.1 events/s) from the periphery to the center of cells in a transverse direction ("T-wave"; ~145 μm/s). Pharmacological interventions and simultaneous recording of membrane potential and Ca^{2+} demonstrated that shear-induced T-waves resulted from action potential (AP)-triggered Ca^{2+} release from the sarcoplasmic reticulum. T-waves were not sensitive to inhibitors of known shear signaling mechanisms except connexin hemichannels and ATP release. Shear stress caused ATP release from these myocytes (~1.1x10^{-17} moles/unit membrane, μm^2); ATP release was increased by enhancement of connexin hemichannels and suppressed by inhibition of the hemichannels, but not affected by inhibitors of other ATP release pathways. Blockade of P2X receptor, but not pannexin or the Na^+–Ca^{2+} exchanger, eliminated shear-induced T-wave initiation. ***Conclusion:*** Our data suggest that shear stress triggers APs and concomitant Ca^{2+} signaling via activation of P2X receptors by connexin hemichannel-mediated ATP release in atrial myocytes.

Introduction

The chambers of the heart are exposed to mechanical stimuli such as stretch, shear stress, and afterload during cardiac cycles, and these stimuli, in turn, affect cardiac excitability and contractility [1, 2]. During each cardiac cycle, cells in the myocardium are exposed to shear stress and become deformed due to interlaminar fluid flow and sliding of the myocardial layers against one other [3, 4]. Under pathological conditions such as valvular diseases, heart failure, or hypertension, atrial volume and pressure overload is implicated in altered

Sun-Hee Woo
Laboratory of Physiology, College of Pharmacy, Chungnam National University
99 Daehak-ro, Yuseong-gu, Daejeon 305-764 (South Korea)
Tel. +82-42-821-5924, Fax +82-42-823-6566, E-Mail shwoo@cnu.ac.kr

atrial excitability [1, 5]. Atria often become enlarged and dilated under such conditions, and the responses of atrial myocytes to stretch, including activation of stretch-activated ion channels (SACs), have been well documented [1, 5, 6]. Under such conditions, mechanical stresses, including shear stress, also increase. In addition, there is clinical evidence that mitral regurgitation or direct irritation by atrial catheters causes atrial arrhythmias without enlargement of the chamber [1, 5]. In cases of chronic mitral regurgitation, the endocardial surface of the atrium is significantly disrupted, directly exposing atrial myocytes to shear stress [7, 8]. However, atrial responses to shear stress remain poorly understood.

A series of recent reports have suggested that cardiac myocytes significantly alter their membrane conductance and Ca^{2+} signaling in response to shear stress [9-14]. It has been reported that shear stress in atrial myocytes enhances Ca^{2+} spark occurrence and induces longitudinal Ca^{2+} waves under resting conditions [9, 12]. The longitudinal Ca^{2+} waves observed in atrial cells under shear stress are completely eliminated by pharmacological blockade of either $P2Y_1$ purinergic signaling or ATP release from atrial cells, and have been abolished by inositol 1, 4,5-trisphosphate receptor type 2 (IP_3R2) knock-out [12]. This suggests that ATP release from atrial myocytes induces longitudinal Ca^{2+} waves by activating $P2Y_1$ receptors. Shear stress-induced Ca^{2+} release from IP_3Rs is thought to play an important role in activation of transient receptor potential melastatin 4 (TRPM4), a Ca^{2+}-activated monovalent cation channel in rat atrial myocytes [13], which may alter membrane conductance.

ATP is released from cardiac myocytes under ischemic and hypoxic conditions, as well as from nerve terminals as a co-transmitter with norepinephrine and acetylcholine [15]. Several mechanical stresses including shear stress have been shown to induce ATP release in various cell types [16-22]. Different cell types selectively use specific ATP release pathway(s) (volume-regulated Cl^- channels [17], maxi anion channels [18], ATP-binding cassette transporters [19], gap junction channels [20, 21], or exocytotic secretion [22]). In atrial myocytes, shear stress-induced longitudinal Ca^{2+} waves were suppressed by inhibition of gap junction hemichannels, but not by inhibition of other ATP release pathways [12]. However, there is no direct evidence of ATP release from atrial myocytes under shear stress.

Shear stress of comparable strength induces a distinct spontaneous Ca^{2+} transient (time-to-peak, T_p: 130 ms) in fura-2-AM-loaded rat atrial myocytes, as shown by epifluorescence measurement [10]. This shear-induced global Ca^{2+} signal occurs faster than longitudinal Ca^{2+} waves in terms of Ca^{2+} release (T_p ≥300 ms). The distinct spatiotemporal properties of shear-triggered Ca^{2+} signals appear to be linked to different mechanisms and Ca^{2+} sources, in that the faster shear-induced epifluorescence Ca^{2+} signal is mediated by mitochondrial Ca^{2+} mobilization [10] unlike the slower IP_3R-mediated longitudinal Ca^{2+} waves [12].

In the present study, we investigated shear-induced Ca^{2+} signaling and the cellular mechanisms underlying shear-mediated global Ca^{2+} waves in single rat atrial myocytes using rapid two-dimensional (2-D) confocal Ca^{2+} imaging, patch clamp method, and ATP chemiluminescence measurements. We applied shear stress to single atrial myocytes using pressurized micro-flow as previously reported [9, 12]. Our data indicate that shear stress causes a global Ca^{2+} wave by triggering action potential (AP) and subsequent L-type Ca^{2+} current (I_{Ca})-induced sarcoplasmic reticulum (SR) Ca^{2+} release, and further suggest that ATP efflux via connexin hemichannels plays an important role in the wave generation via P2X receptor activation.

Materials and Methods

Isolation of atrial myocytes

Atrial myocytes were enzymatically isolated from male Sprague-Dawley rats (200–300 g, total 69 rats) as previously described [12]. This study conforms with the Guiding Principles for the Care and Use of Experimental Animals published by the Korean Food and Drug Administration and Animal and Plant Quarantine Agency in South Korea. The experimental protocols were approved by the Animal Care and Use Committees of the Chungnam National University, South Korea (No. CNU-00368). Rats were deeply

anesthetized with pentobarbital sodium (150 mg/kg, *i.p.*), the chest cavity was opened, and hearts were excised. The excised hearts were retrogradely perfused at 7 ml/min through the aorta (at 36.5°C), first for 3 min with Ca^{2+}-free Tyrode solution composed of (in mM) 137 NaCl, 5.4 KCl, 10 HEPES, 1 $MgCl_2$, and 10 glucose, pH 7.3, and then with Ca^{2+}-free Tyrode solution containing collagenase (1.4 mg/ml; Type A (*EC 3.4.24.3*), Roche) and protease (0.14 mg/ml; Type XIV (*EC 3.4.24.31*), Sigma, St. Louis, MO, USA) for 12 min; and finally with Tyrode solution containing 0.2 mM $CaCl_2$ for 5 min. The atria of the digested heart were then cut into several sections and subjected to gentle agitation to dissociate the cells. The freshly dissociated cells were stored at room temperature in Tyrode solution containing 0.2 mM $CaCl_2$.

Application of shear stress

Pressurized flows of external solutions were applied onto the single myocytes through a microbarrel (internal diameter = 250 μm) the tip of which was placed at ≈150 μm from the cell and was connected to a fluid reservoir with 40-cm heights [9, 12]. The shear stress (dyn/cm^2) was calculated for flow in cylindrical tubes according to the equation [23]:

Shear stress = $4\mu Q / \pi r^3$,

where μ represents the fluid viscosity ($1.002 \cdot 10^{-2}$ dyn·s/cm^2 for water), Q is the flow rate (cm^3/s), and r is the internal radius (cm) of the microbarrel. The micro-flow system generated shear stress of ~16 dyn/cm^2 (equal to 0.16 N/m^2) at 40-cm reservoir height. This shear strength appeared to be maximum to consistently generate global Ca^{2+} waves in atrial myocytes. The positioning of the microbarrel was performed under microscope using a micromanipulator (Prior England 48260). The experimental cells were attached to the bottom of the chamber without a coating material. Using a microscope and video monitor, it was confirmed that no movement of the cell occurred during the fluid puffing before the start of the experiments.

To measure ATP releases from atrial myocytes using luciferin-luciferase assay shear stress was applied to fields of cells in a laminar flow chamber (VC-LFR-18-SS, C&L Instruments, USA) connected to the solution reservoirs. The shear stress was calculated using the equation:

Shear stress = $6\mu Q / bh^2$,

where μ and Q have the same meaning as above, b represents the chamber width (cm), and h is the chamber height (cm). For this flow chamber, a flow rate of 0.5, 2, 4 and 8 ml/min generates a shear stress of 1, 4, 8 and 16 dyn/cm^2 respectively.

2-D confocal Ca^{2+} imaging

To measure intracellular Ca^{2+} signals, myocytes were loaded with 3 μM fluo-4 acetoxymethyl (AM) ester (Invitrogen, USA) for 30 min. The dye-loaded cells were continuously superfused with 2 mM Ca^{2+}-containing normal Tyrode solution (see above; pH 7.4). Intracellular Ca^{2+} fluorescence was imaged at 60 Hz in 2-D using a laser scanning confocal imaging system (A1, Nikon) attached to an inverted microscope (Eclipse Ti, Nikon) fitted with a x60 oil-immersion objective lens (Plan Apo, Numerical Aperture 1.4, Nikon). Dyes were excited at 488 nm using Ar laser (Omnichrome) and fluorescence emission at >510 nm was detected. Images were recorded by an workstation software, NIS Elements AR (v3.2, Nikon).

To assess shear-induced Ca^{2+} wave propagating from the cell periphery to the center in the transverse direction, local Ca^{2+} changes from both peripheral and centermost regions of 2-D Ca^{2+} images were analyzed (see the Region-Of-Interest [ROI] in the insets of figures in ref [24]). Global Ca^{2+} waves, showing time-to-90% of peak ($T_{p,90}$) of peripheral Ca^{2+} releases less than 35 ms were counted. In order to estimate Ca^{2+} increases, the average resting fluorescence intensity (F_0) was calculated from several frames immediately before application of shear stress. Tracings of local Ca^{2+} signals were shown as the average fluorescence of each ROI normalized relative to the F_0 (F/F_0).

Simultaneous measurement of membrane potential and Ca^{2+} images

To measure membrane potential simultaneously with confocal Ca^{2+} signals the fluo-4 AM (3 μM, 30 min)-loaded cell was whole-cell patch clamped in a current clamp mode using an EPC7 plus amplifier (HEKA Elektronik, Lambrecht/Pfalz, Germany). The patch pipettes were made of glass capillaries (Kimble Glass Inc., Vineland, NJ, USA) with a resistance of ~3 MΩ when filled with the internal solutions containing (in mM): 130 KOH, 130 Glutamic acid, 7 KCl, 1 MgCl2; 10 HEPES, 5 MgATP, 0.1 GTP, 0.02 EGTA, 0.1 fluo-3-K_5; pH = 7.2. Measurement of membrane potential was generally carried out 6-7 min after the rupture. The same confocal system was used (see above) and was synchronized with patch clamp system using a trigger module in the

confocal system. Generation of the current-clamp protocol and acquisition of the data were carried out using pClamp PC program (v10.7, Molecular Devices, Foster City, CA, USA) via an A/D converter (Digidata 1550B; Molecular Devices). The voltage signals were filtered at 10 kHz before digitization and storage. The traces were analyzed using Clampfit software (v10.7) and OriginPro program (v8, SR0, OriginLab Corp., Northampton, MA, USA). The experiments were performed at room temperature (22-25°C).

Measurement of ATP release using chemiluminescence assay

ATP release from atrial myocytes was measured by chemiluminescence detection using luciferin-luciferase reaction (ATP Bioluminescence Assay Kit HS II, Roche Diagnostics GmbH, Sandhofer Strasse Mannheim, Germany). With exposing atrial cells to shear stress, outflow from the shear chamber was collected for 10 s at 2-s intervals. The collected solutions were subjected to the ATP-driven luciferin-luciferase reaction and then the intensity of luminescence was detected at 562 nm using a luminometer (EnVision 2101 Multilabel Reader, Perkin Elmer, Waltham, MA, USA). ATP standard curve was derived using eight standard ATP solutions (1 pM ~ 10 μM) and the same detection method.

The concentration of ATP was estimated as moles/unit cell membrane area. To derive this value, the numbers of live cells attached onto the bottom of shear chamber were counted off-line using their pictures. Total membrane area from each experimental batch was derived using approximate cell surface area and the number of cells counted. For this calculation, we assumed that atrial cells were cuboid.

Chemicals

Reagents used to make Tyrode solutions, and 2-aminoethoxydiphenyl borate (2-APB), apyrase, carbenoxolone, $CdCl_2$, $GdCl_3$, diphenyleneiodonium (DPI), $NiCl_2$, nifedipine, probenecid, suramin and tetrodotoxin (TTX) were purchased from Sigma-Aldrich. 9-phenanthrol, KB-R7943, MRS-2179 and pyridoxalphosphate-6-azophenyl-2',5'-disulfonic acid (iso-PPADS) were supplied by Tocris Bioscience (Avonmouth, Bristol, BS11 9QD, UK). Fluo-4 AM and fluo-3 K_5 were from Thermo Fisher Scientific (Waltham, MA, USA). Ryanodine and U73122 were purchased from Calbiochem (Merck Millipore Corporation, Darmstadt, Germany). GsMTx-4 was obtained from Alomone Labs (Jerusalem, Israel).

Statistics

The numerical results are presented as means ± standard error of the mean (S.E.M.). *n* indicates number of cells used. Paired or unpaired Student's *t*-tests were used for statistical comparisons depending on the experiments. Differences at $P<0.05$ were considered to be statistically significant.

Results

Shear stress induces AP and a subsequent global Ca^{2+} wave in atrial myocytes

Fig. 1A shows a representative global Ca^{2+} wave induced by exposure to shear stress (~16 dyn/cm^2) in rat atrial myocytes. These waves generally showed fast Ca^{2+} release from the entire cell periphery and propagated into the cell interior in a transverse direction. The average speed of such Ca^{2+} waves was 144 ± 17.2 μm/s (at 60 Hz; n=17). One Ca^{2+} wave was generally observed for each 10-s shear application (0.12 ± 0.01 events/s, n=61). The latency of these shear-triggered (for 8–20 s) waves varied among myocytes (0.8–17 s; 6.0 ± 0.53 s, n=85). The shear-induced Ca^{2+} wave re-occurred in individual cells upon repeated shear application with an interval of 4–5 min.

The average local Ca^{2+} release from the periphery (red trace) was significantly faster and larger (Fig. 1B inset graph; $T_{p,90}$, 27 ± 3.9 ms; $\Delta F/F_0$, 1.70 ± 0.14) than central Ca^{2+} release (green trace; $T_{p,90}$, 66 ± 3.9 ms, $P<0.05$; $\Delta F/F_0$, 1.06 ± 0.15, $P<0.05$, n=61). The spatiotemporal properties of local Ca^{2+} release appeared similar to those of depolarization-triggered Ca^{2+} waves in atrial myocytes [24-27] lacking transverse tubules [28]. Therefore, we next used TTX, a blocker of voltage-dependent Na^+ channels, to inhibit the upstroke of APs. After cells were treated with 10 μM TTX for 30 s, shear exposure no longer triggered Ca^{2+} waves (Fig. 1A-C), although background Ca^{2+} levels were slightly increased by shear exposure (Fig. 1B and D). This TTX-sensitive Ca^{2+} wave traveling from the cell periphery to the center in a

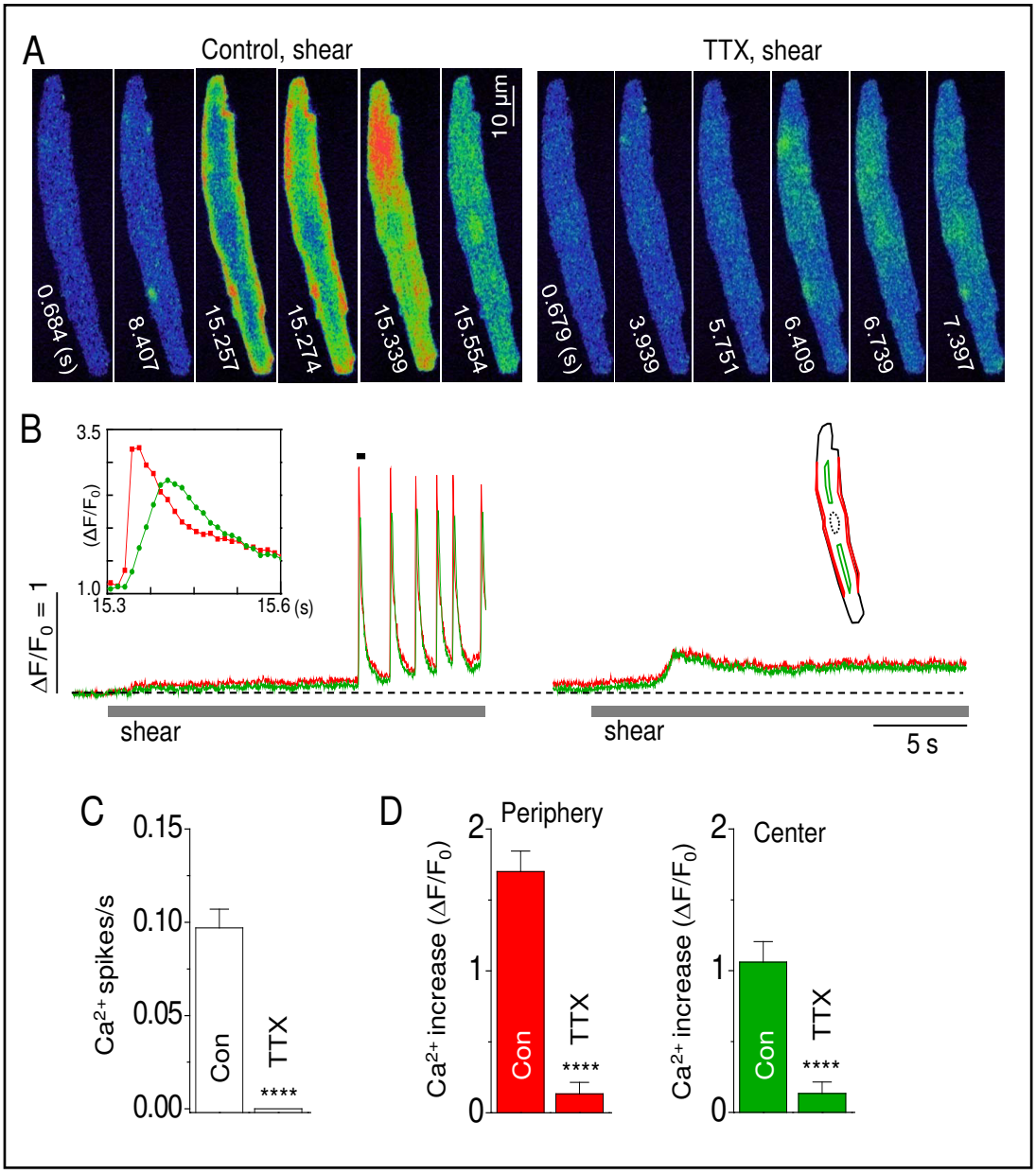

Fig. 1. Tetrodotoxin-sensitive global Ca^{2+} wave induced by shear stress in atrial myocytes. A: series of 2-D confocal Ca^{2+} images recorded during the periods indicated by the black bars above the Ca^{2+} traces in the panel B, showing a shear stress (16 dyn/cm^2)-induced global Ca^{2+} wave propagating from the periphery to the center in a representative rat atrial myocyte (left) and its sensitivity to tetrodotoxin (TTX, 10 μM), the voltage-gated Na^+ channel blocker (right). Time, indicated in each image, represents the time when the image was selected during the whole recording period (panel B). B: Ca^{2+} signal traces measured at 60 Hz from the peripheral (red) and central (green) domains in the confocal cell Ca^{2+} images (right panel, inset). Inset graphs: expanded time course for the selected period marked by the black bar above the Ca^{2+} trace. C: averaged frequency of shear-induced T-waves in the absence (Con) and presence of TTX. D: comparison of peripheral and central Ca^{2+} increases during shear stress before and after the treatment of TTX. Con, n=61. TTX, n=5. $^{****}P<0.0001$ vs. Con (unpaired t-test).

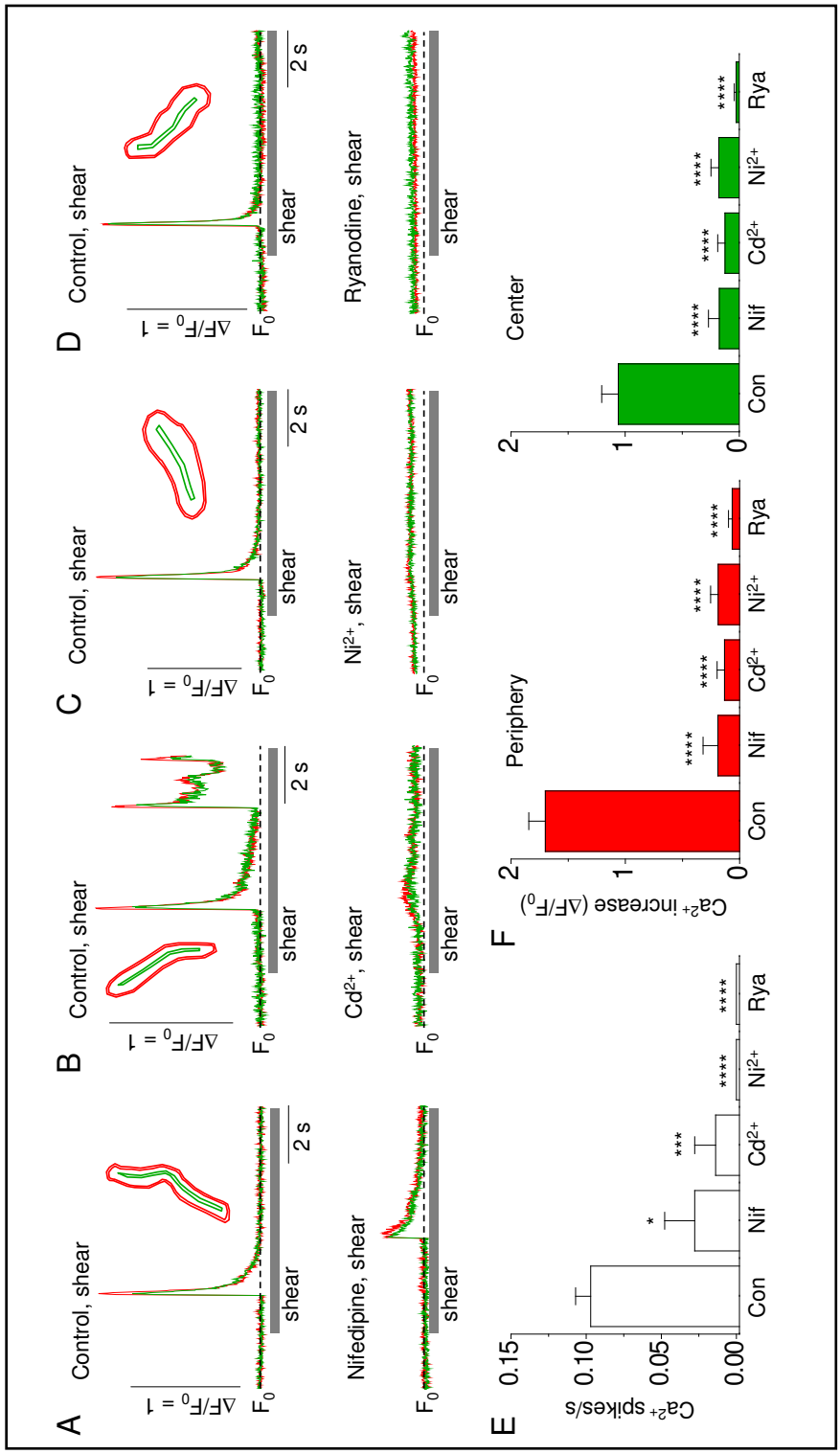

Fig. 2. Shear-induced T-wave represents I_{Ca}-triggered Ca^{2+} release from the SR. A–D: peripheral and central Ca^{2+} signals in the representative cells associated with shear (16 dyn/cm^2)-induced T-waves under control conditions (upper traces) and after applications of nifedipine (15 μM, 5 s), Cd^{2+} (50 μM, 10 s), Ni^{2+} (5 mM, 5 s) or ryanodine (10 μM, 4 min) (lower traces). Data shown in each panels were recorded in the same atrial myocytes. Right insets represent ROIs used to measure the local Ca^{2+} signals. E: averaged frequency of shear-induced T-waves (Ca^{2+} spikes), measured under control conditions (Con, n=61) and after the applications of nifedipine (Nif, n=7), Cd^{2+} (n=4), Ni^{2+} (n=5) or ryanodine (Rya, n=5). *P<0.05, ***P<0.001 vs. Con. F: comparison of local Ca^{2+} increases by shear stress in the absence and presence of the interventions. ****P<0.0001 vs. Con (unpaired t-test).

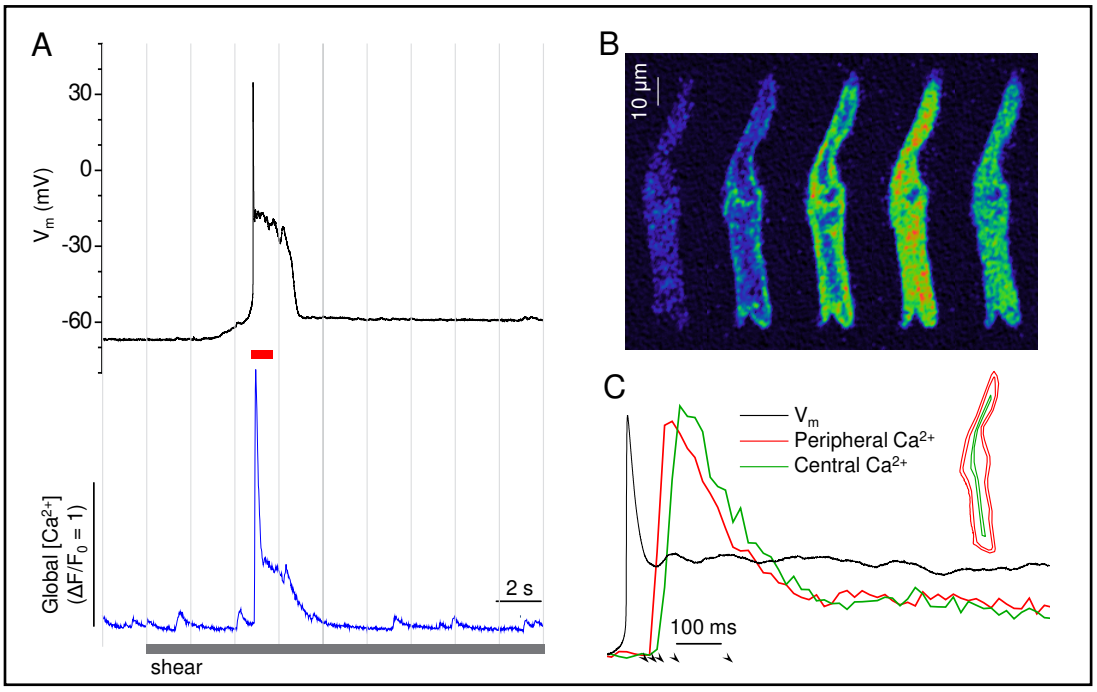

Fig. 3. Shear stress-induced action potential (AP) and subsequent T-wave in atrial myocyte. A: simultaneous recording of AP and global Ca^{2+} signal associated with T-wave in a representative atrial myocyte during shear stress exposure (16 dyn/cm^2). B: confocal Ca^{2+} images recorded at the time pointes sequentially marked by the arrowheads underneath the expanded local Ca^{2+} traces in the panel C. C: superimposed AP (black) and local Ca^{2+} signals from the cell periphery (red) and center (green) of the cell Ca^{2+} images (see ROI) during the period marked by the red bar in the panel A, showing AP occurrence prior to the onset of T-wave under shear stress.

transverse direction termed 'T-wave' under shear stress was distinguished from previously reported shear stress-induced longitudinal Ca^{2+} waves in atrial myocytes by its spatiotemporal properties and mechanism [12].

We further examined whether shear-triggered T-waves are mediated by I_{Ca}-induced Ca^{2+} release using blockers of I_{Ca} and ryanodine receptors (RyRs). Fig. 2 A-D shows peripheral and central Ca^{2+} transients associated with shear-triggered T-waves, under control conditions (upper traces) and with suppression of I_{Ca} (15 µM nifedipine for 15 s; 50 µM Cd^{2+} or 5 mM Ni^{2+} for 5-10 s) or RyRs (10 µM ryanodine) (lower traces). Fig. 2 E and F summarize the average frequency of shear-induced T-waves and local Ca^{2+} release with and without these interventions. A few cells showed fast Ca^{2+} spikes with much less Ca^{2+} released in the presence of 15 µM nifedipine (Fig. 2 E and F, "nif"). Ni^{2+} at a concentration of 5 mM also blocks Na^+–Ca^{2+} exchange (NCX), which might have increased basal Ca^{2+} slightly (Fig. 1C, lower trace; $\Delta F/F_0$: periphery, 0.09 ± 0.02, P<0.01; center, 0.10 ± 0.02, P<0.01; n=5). Ryanodine independently increased basal Ca^{2+} levels ($\Delta F/F_0$: periphery, 0.10 ± 0.02, P<0.01; center, 0.10 ± 0.02, P<0.01; n=5), which may be due to subconductance state of RyRs caused by ryanodine [29]. Another RyR inhibitor, tetracaine (1 mM), also completely abolished wave occurrence (data not shown). These results suggest that shear-induced T-waves represent I_{Ca}-triggered SR Ca^{2+} release associated with APs.

To confirm this hypothesis we simultaneously recorded Ca^{2+} signals and membrane potential under shear stress using confocal imaging and whole-cell patch clamp, respectively. We observed that shear stress produced graded depolarization followed by AP and a subsequent T-wave (Fig. 3). Shear stress-triggered APs were significantly prolonged at –15 ~ –30 mV in most of the cells tested, and were accompanied by long-lasting Ca^{2+} release (Fig. 3A). The mean resting membrane potential and average amplitude of shear-triggered APs

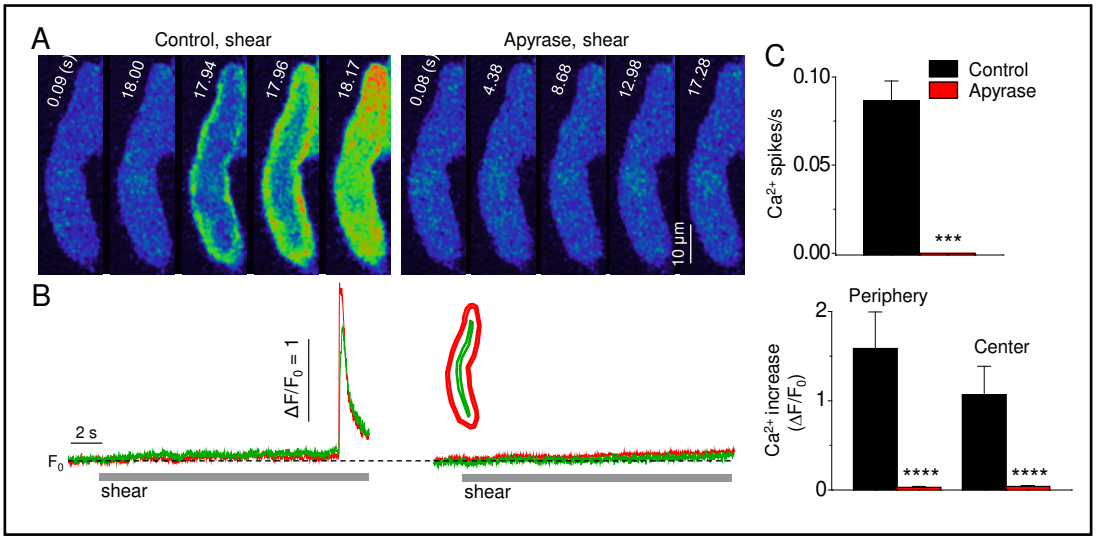

Fig. 4. Potential role of ATP release in generation of T-wave under shear stress. A: series of confocal Ca^{2+} images showing shear (16 dyn/cm^2)-induced T-wave under control condition and its sensitivity to the external ATP metabolizing enzyme apyrase (2 U ml^{-1}; D) in a representative atrial myocyte. B: Ca^{2+} signals measured at 60 Hz from the peripheral (red) and central (green) ROIs (inset) from the cells shown above the traces. C: averaged frequency of shear-induced T-wave occurrence (upper) and mean shear-mediated Ca^{2+} increase (lower) in the absence and presence of apyrase (n=5). $^{***}P<0.001$, $^{****}P<0.0001$ vs. Control (paired t-test).

were −69.9 ± 2.46 mV and 116 ± 2.81 mV (n=8), respectively. The duration of shear-induced APs varied from 200 to 3000 ms at −50 mV. Variation was observed between cells as well as between APs recorded in the same cell.

Possible role of ATP release and connexin hemichannels in shear-induced T-wave generation

Our previous Ca^{2+} imaging experiments using pharmacological interventions have shown evidence that atrial cells may release ATP through gap junction hemichannel under shear stress and activate $P2Y_1$ receptors [12]. Atrial myocytes also express ionotropic P2X receptors that can be activated by ATP and depolarize the cell membrane under resting conditions [15, 30]. To test this hypothesis we first used the external ATP-metabolizing enzyme apyrase to reduce the level of released ATP. After treatment with apyrase (2 U/ml, 30 min), shear-triggered T-waves were no longer observed in cells that had produced such wave under control conditions (Fig. 4 A-C). Increases in local Ca^{2+} levels under shear stress were completely suppressed by apyrase exposure (Fig. 4C, lower).

We next examined whether gap junction hemichannels play a role in the generation of T-waves under shear stress. To suppress hemichannels, cells were pre-treated with carbenoxolone (50 µM, 10 min). After treatment with this chemical, shear stress failed to induce T-waves (Fig. 5 A-C). We did not observe significant background Ca^{2+} increases due to shear stress in the presence of carbenoxolone (Fig. 5C, lower). Carbenoxolone (50 µM) can affect connexin- and pannexin-gap junction channels. Although connexins are major gap junction channels in cardiac myocytes, pannexin expressed in cardiac myocytes may also release ATP [21, 31] and promote arrhythmogenic activity [32]. Therefore, we examined whether pannexins play a role in shear-triggered Ca^{2+} waves, using probenecid, a selective inhibitor of pannexins that does not affect connexins at concentrations up to 1 mM [33]. We found that exposure to 800 µM probenecid had no effect on either generation of T-waves or on local Ca^{2+} increases under shear stress (Fig. 5D-F). Treatment with probenecid alone caused significant increase in the basal Ca^{2+} level (Fig. 5E; $\Delta F/F_0$: periphery, 0.16 ± 0.02, $P<0.05$; center, 0.20 ± 0.02, $P<0.05$; n=4).

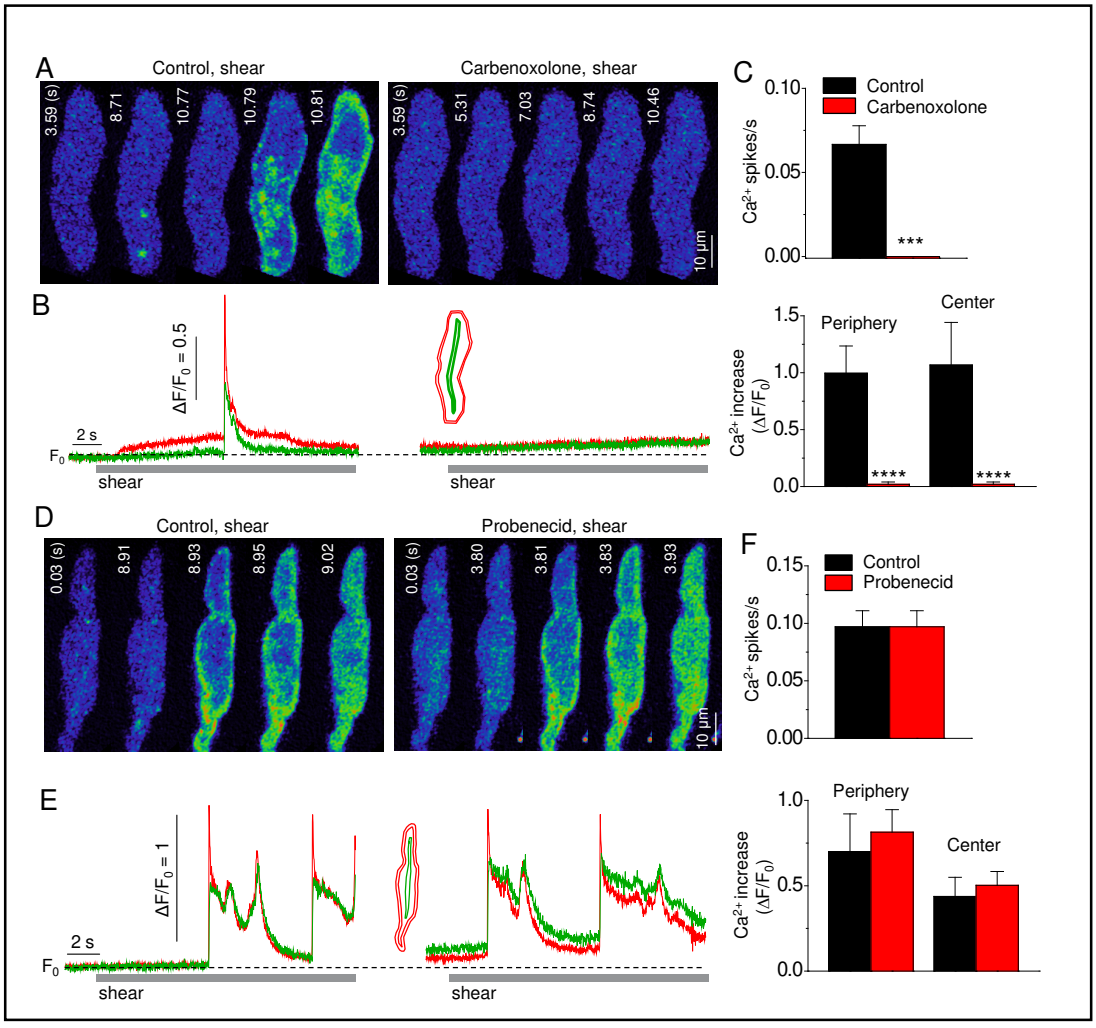

Fig. 5. Role of connexin hemichannels in generation of T-wave under shear stress. A and D: series of confocal Ca^{2+} images showing shear (16 dyn/cm^2)-induced T-wave under control condition and in the presence of gap junction hemichannel blocker carbenoxolone (50 μM) (A) or pannexin inhibitor probenecid (800 μM) in atrial myocytes. B and E: Ca^{2+} signals measured at 60 Hz from the peripheral (red) and central (green) domains (inset) from the cells shown above the traces. C and F, averaged frequency of shear-induced T-waves (upper) and mean shear-mediated Ca^{2+} increase (lower) in the absence and presence of carbenoxolone (C, n=5) or probenecid (F, n=4). $^{***}P<0.001$, $^{****}P<0.0001$ vs. Control (paired t-test).

Potential role of P2X receptors in the generation of T-wave under shear stress

To further test our hypothesis, we next examined whether the P2 receptor inhibitor suramin affects the occurrence of T-waves under shear stress. Pretreatment with suramin (10 μM; 12) for 5 min completely suppressed the occurrence of T-waves upon shear stimulus (Fig. 6A-C), supporting a role of P2 receptors in shear-induced T-wave generation. We further investigated a possible role of the P2X receptor in initiation of T-wave under shear stress using the P2X receptor antagonist iso-PPADS [34, 35]. In nine out of fourteen cells that showed shear-induced T-waves without treatment, shear exposure failed to induce T-wave after application of 6 μM iso-PPADS (by 76.4 ± 9.2%). In the presence of 30 μM iso-PPADS, shear stress no longer triggered T-waves (Fig. 6D-F). The averaged magnitude of local Ca^{2+} increase induced by shear stimulation was significantly reduced by iso-PPADS (Fig. 6F). After withdrawal of iso-PPADS, shear-induced T-waves were observed again in some cells (data not shown). These results indicate that shear stress initiates T-waves mainly via autocrine activation of P2X receptors.

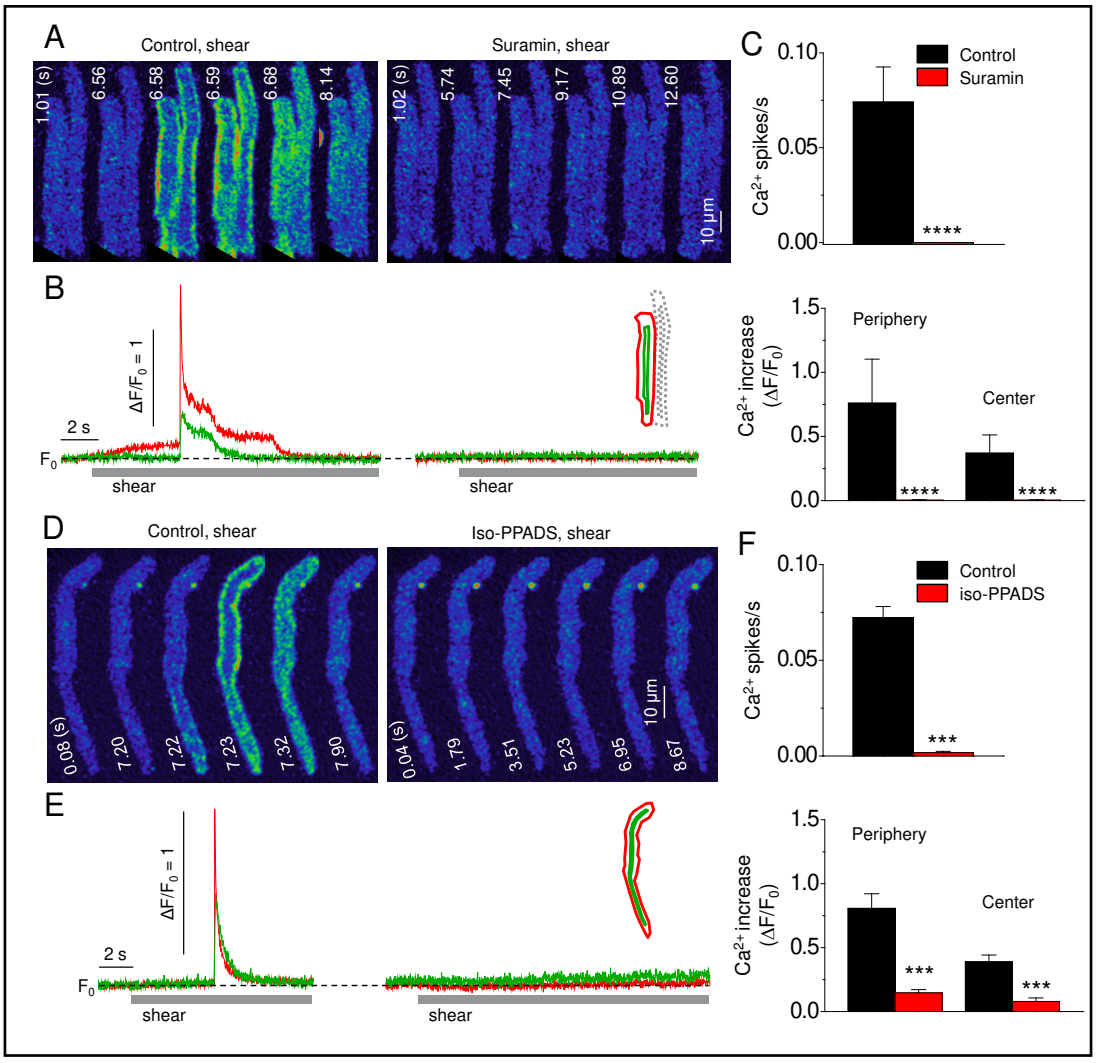

Fig. 6. Role of P2X receptors in initiation of T-wave under shear stress. A and D: series of confocal Ca^{2+} images showing shear (16 dyn/cm^2)-induced T-waves under control conditions and its sensitivity to the antagonists of P2 (10 μM suramin; A) or P2X purinoceptors (30 μM Iso-PPADS; D) in the representative atrial myocytes. B and E: Ca^{2+} signals measured at 60 Hz from the peripheral (red) and central (green) regions (inset) from the cells shown above the traces. C and F: averaged frequency of shear-induced T-waves (upper) and mean shear-mediated Ca^{2+} increase (lower) in the absence and presence of either suramin (C, n=5) or Iso-PPADS (F, n=9). ***P<0.001, ****P<0.0001 vs. Control (paired t-test).

No role of SAC, nicotinamide adenine dinucleotide phosphate oxidase (Nox), and $P2Y_1$ purinergic signaling in shear-induced T-wave generation

We additionally tested whether shear-induced autocrine activation of the $P2Y_1$ receptor–PLC–IP_3R2 signalling pathway contributes to generation of T-waves upon shear stimulation using pharmacological interventions. Blockers of the $P2Y_1$ receptor (MRS-2179, 0.2 μM), PLC (U73122, 5 μM), and IP_3R (2-APB, 3 μM) neither suppressed the occurrence of shear-induced T-wave (Fig. 7 A-C, and G) nor altered Ca^{2+} releases associated with the T-waves (Fig. 7H). These results suggest that $P2Y_1$ signalling does not mediate the generation of shear-induced T-waves.

Because shear stress can induce local membrane stretch, we tested whether SACs and Nox, the key signalling molecules activated by stretch [36, 37], play a role in this shear response. In cells producing shear-induced T-waves, we examined the effects of the SAC blocker GsMTx-4 (3 μM) and the Nox inhibitor DPI (3 μM) on the occurrence of shear-induced

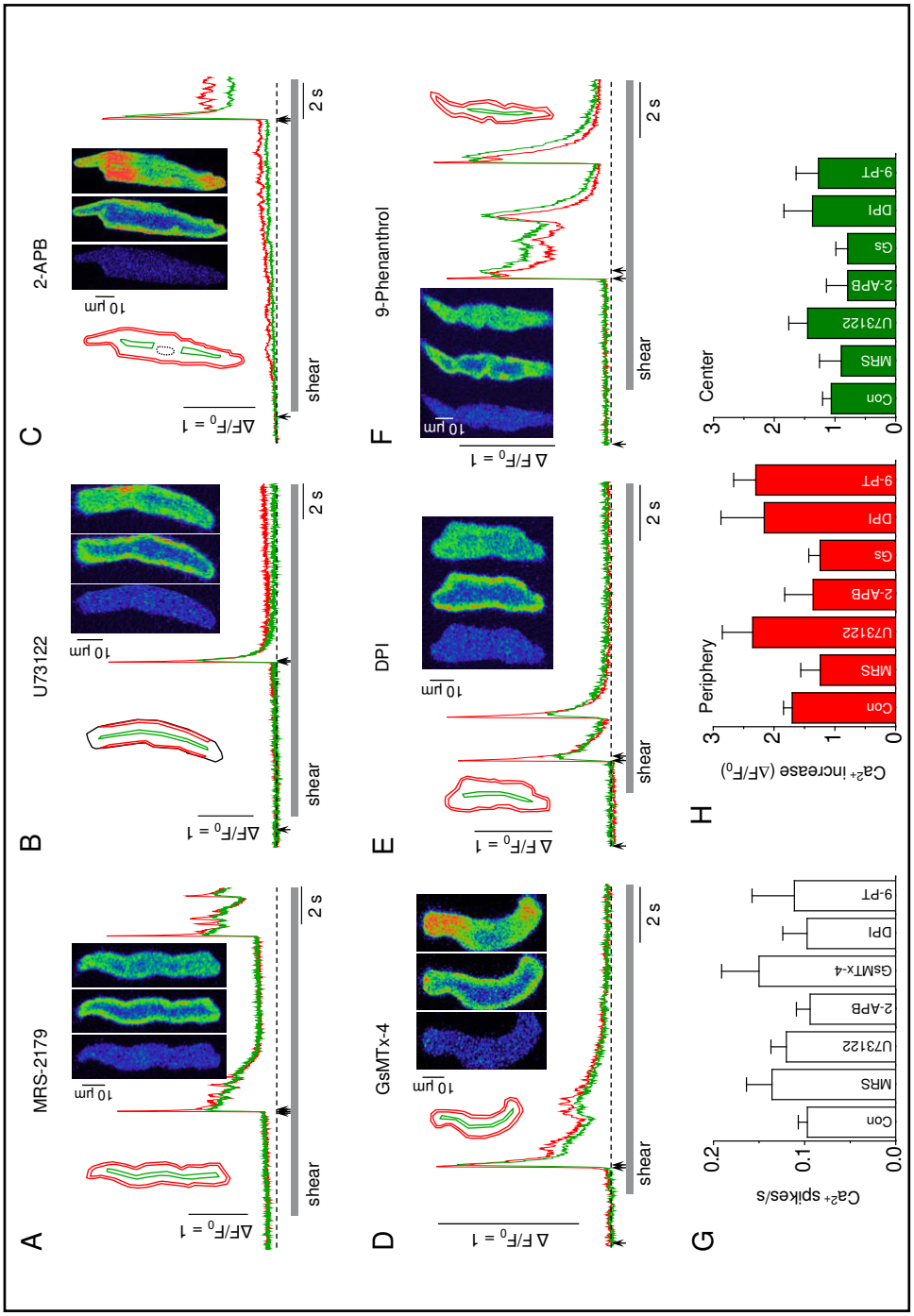

Fig. 7. No role of $P2Y_1$ purinoceptor signaling, SAC, Nox, and TRPM4 in generation of T-wave under shear stress. Local Ca^{2+} signals from the periphery (red) and center (green) of the representative cells, pretreated with $P2Y_1$ antagonist (0.2 μM MRS-2179; A), PLC inhibitor (5 μM U7312; B), IP_3R inhibitor (3 μM 2-APB; C), SAC blocker (3 μM GsMTx-4; D), Nox inhibitor (3 μM DPI; E) or TRPM4 blocker (10 μM 9-phenanthrol; F), showing continued generation of shear-induced T-waves in the presence of these chemicals. Insets in the left side of each panel show ROIs used to measure the local Ca^{2+} signals. Confocal Ca^{2+} images displaying T-wave generated under shear stress were illustrated in the right side of each panel. Arrows underneath the Ca^{2+} trace in each panel indicate the time points when the images were recorded. Dotted lines indicate the basal Ca^{2+} level (F_0) measured under control conditions before the interventions. G and H: averaged frequency of shear-triggered T-waves (G) and mean Ca^{2+} increases by shear stress (H) in the absence (Con, n=61) and presence of MRS-2179 (n=9), U73122 (n=5), 2-APB (n=5), GsMTx-4 (n=4), DPI (n=4), or 9-phenanthrol (n=5) (unpaired t-test).

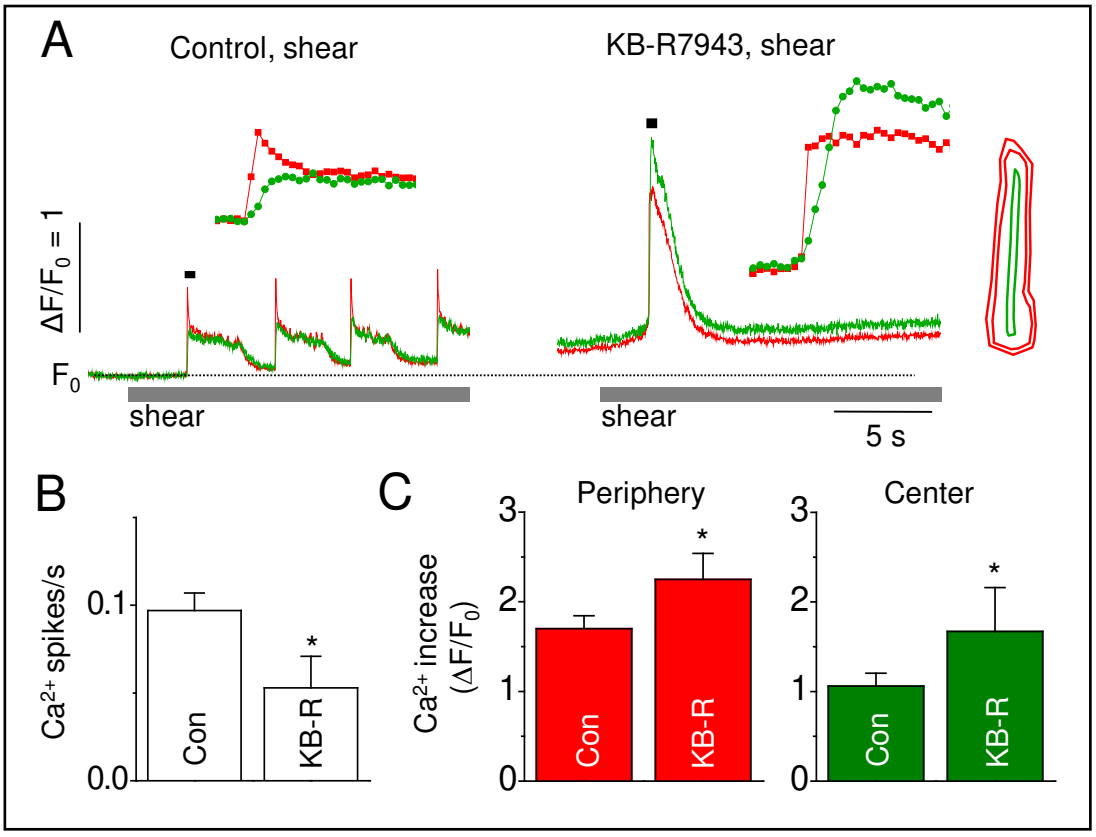

Fig. 8. Potential role of NCX in facilitation of T-waves under shear stress. A: shear (16 dyn/cm^2)-induced local Ca^{2+} transients associated with T-waves in the absence (Control) and presence of the inhibitor of NCX KB-R7943 (0.2 μM) in the same atrial cell. Inset cell diagram shows peripheral and central ROIs used to measure the local Ca^{2+} signals. Inset Ca^{2+} traces represent expanded traces for the period marked by black bar above each trace. The period of shear stress application was indicated by the gray bar under the local Ca^{2+} signals. B: averaged frequency of shear-induced T-waves under control conditions (Con, n=61) and after application of KB-R7943 (KB-R, n=6). *P<0.05 vs. Con. C: comparison of shear-triggered local Ca^{2+} increases before (Con) and after application of KB-R7943 (n=6, *P<0.05 vs. Con, unpaired t-test).

Ca^{2+} waves. Neither inhibitor affected the frequency of shear-induced T-waves (Fig. 7D, E and G). In addition, the magnitude of shear-induced local Ca^{2+} increase was not changed by pre-treatment with GsMTx-4 or DPI (Fig. 7H).

Shear stress activates non-selective cation currents through TRPM4 channels via IP_3R2-induced Ca^{2+} release in atrial myocytes [13]. We tested whether TRPM4 channels contribute to T-wave activation under shear stress using the TRPM4 blocker 9-phenanthrol. At concentrations ≤10 μM, 9-phenanthrol has been shown not to affect the I_{Ca} in cardiac myocytes [38]. Pre-treatment with 10 μM 9-phenanthrol did not alter the frequency of T-waves (Fig. 7F and G) or local Ca^{2+} increases under shear stress (Fig. 7H).

Facilitation of T-wave occurrence by NCX under shear stress

Triggered activity can be induced by NCX-mediated inward current in cardiac myocytes [39]. Therefore, we examined the potential role of NCX in generation of T-waves under shear stress. When atrial cells were pretreated with the NCX inhibitor KB-R7943 at a concentration of 0.2 μM [39], they continued to show shear-induced T-waves (Fig. 8A and B). KB-R7943, at the concentration of 0.2 μM, did not affect I_{Ca} (data not shown). Interestingly, KB-R7943 suppressed repetition of T-waves under shear stress (Fig. 8A), resulting in a lower frequency of T-waves (Fig. 8B). Shear-induced Ca^{2+} transients under NCX inhibition were larger and prolonged, with more prominent increases in central Ca^{2+} compared with peripheral Ca^{2+}

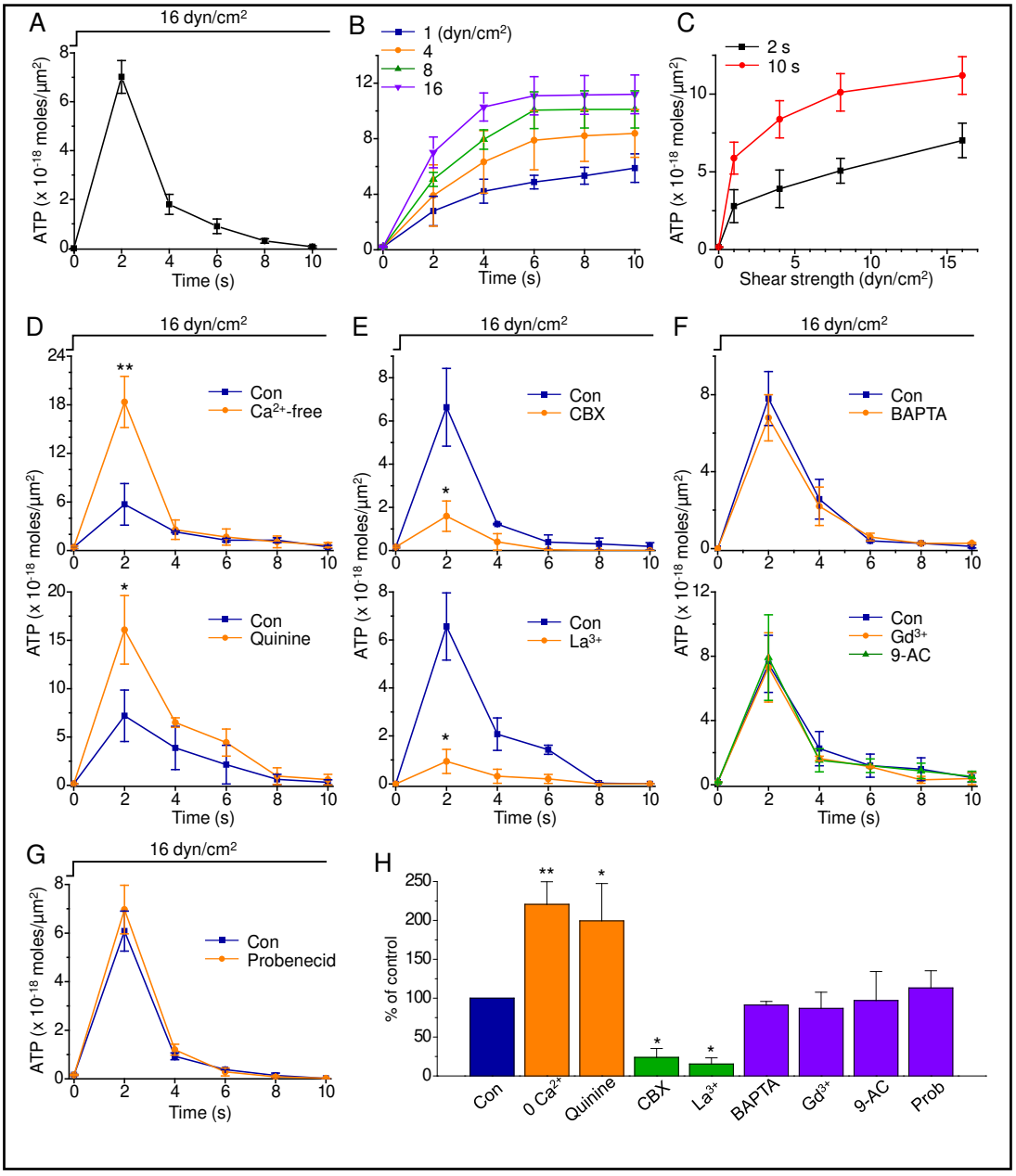

Fig. 9. Shear stress induces ATP release from isolated rat atrial myocytes through connexin hemichannels. A: the amount of ATP release per unit membrane area (μm^2) of atrial myocytes under 10-s long shear application (24 different experimental cell batches). B and C: cumulative ATP released under the application of different shear forces (1, 4, 8, and 16 dyn/cm^2) for 10 s, showing dependence of ATP release on the shear strength (1, 4, and 8 dyn/cm^2: 6 batches; 16 dyn/cm^2: 24 batches). D: shear-induced ATP release was increased by Ca^{2+}-free solution (5 experiments) and quinine (100 μM; 4 experiments) that enhance connexin hemichannel function ($^{**}P<0.01$, $^{*}P<0.05$ vs. Con). E: suppression of shear-induced ATP release after incubation of atrial myocytes with gap junction blockers carbenoxolone (CBX, 50 μM, 7 batches) and La^{3+} (2 mM) ($^{*}P<0.05$ vs. Con, 5 batches). F: No effect of exocytosis inhibition (10 μM BAPTA-AM, 4 batches), maxi anion channel blockade (50 μM Gd^{3+}, 3 batches), or Cl^- channel inhibition (1 mM 9-AC, 6 batches) on shear-induced ATP release. G: shear-induced ATP release was not suppressed by pannexin inhibition 800 μM probenecid (5 batches). H: Comparison of the effects of the interventions on shear-induced ATP releases relative to the level of ATP release under control conditions. $^{**}P<0.01$, $^{*}P<0.05$ vs. Con.

(Fig. 8A and C). This finding might be related to enhanced regenerative and cooperative Ca^{2+} releases from the non-junctional Ca^{2+} release sites caused by slower removal of peripheral Ca^{2+}. These results suggest that NCX at least partially contributes to T-wave generation under shear stress, but that NCX is not absolutely required for the initiation of shear-induced T-wave.

Shear-induced ATP release from atrial myocytes through connexin hemichannels

In the next series of experiments, we directly measured ATP release from atrial myocytes under shear stress using the luciferin-luciferase reaction that generates luminescence in an ATP-dependent manner. ATP-induced chemiluminescence was measured from external solutions collected for 10-s shear application at 2-s intervals. ATP level was increased upon shear stress stimulus of 16 dyn/cm^2, reaching a peak value of (7.02 ± 0.67)x10^{-18} moles per unit membrane area (μm^2) at 2 s (24 batches; Fig. 9A). The total amount of ATP released for a 10-s application of 16 dyn/cm^2 shear stress, measured from plots of cumulative ATP versus the duration of shear exposure (Fig. 9B), was (11.2 ± 1.21)x10^{-18} moles/μm^2 (24 batches; Fig. 9B). ATP release increased in a shear strength-dependent manner (Fig. 9B and C).

We further examined the mechanism of ATP release in rat atrial myocytes under shear stress using pharmacological interventions. Removal of the external Ca^{2+} that enhances connexins [40] increased shear-induced ATP release to ~2.2-fold (Fig. 9D and H). Consistently, pretreatment with the gap junction enhancer quinine (100 μM) significantly increased shear-induced ATP release (~2 fold, Fig. 9D and H). Inhibition of gap junction hemichannels using either carbenoxolone (50 μM) or La^{3+} (2 mM) suppressed shear-induced ATP release by 75-85% (Fig. 9E and H). Contributions of other ATP release pathways [17-22] under shear stress were also assessed. When exocytosis, a Ca^{2+}-dependent process, was suppressed by chelating intracellular Ca^{2+} using BAPTA-AM (10 μM), ATP release under shear stress was unaltered (Fig. 9F and H). Pretreatment with either the Cl^- channel inhibitor 9-anthracenecarboxylic acid (1 mM) or the maxi anion channel inhibitor Gd^{3+} (50 μM [18]) did not alter shear-induced ATP release (Fig. 9F and H). Blockade of pannexins using probenecid (800 μM) did not affect shear-mediated ATP release (Fig. 9G and H). Fig. 9H summarizes shear-induced ATP release under different experimental interventions relative to that under control conditions. These results suggest that shear stress-induced ATP release may be mediated by connexin hemichannels in atrial myocytes.

Discussion

Here, we report new evidence suggesting that shear stress induces ATP efflux from atrial myocytes through connexin hemichannels, and that released ATP, in turn, triggers AP coincident with global Ca^{2+} wave via activation of P2X receptors. The AP was observed prior to the occurrence of Ca^{2+} wave under shear stress (Fig. 3). In addition, the suppression of voltage-dependent Na^+ or Ca^{2+} channels, or RyRs eliminated the shear-induced Ca^{2+} wave generation (Fig. 1 and 2). Initiation of such Ca^{2+} wave under shear stress was completely suppressed by blockade of either cellular ATP release (apyrase; Fig. 4) or P2X receptors (Fig. 6D-F). Inhibition of SAC, Nox, TRPM4, $P2Y_1$ receptor–PLC–IP_3R signaling, or pannexins did not suppress generation of T-waves under shear stress (Fig. 7). Inhibition of NCX only partially reduced T-wave occurrence, without blocking wave initiation (Fig. 8). Assessment of ATP release from atrial myocytes under shear stress combined with pharmacological interventions demonstrated an important role of connexin hemichannels in ATP release from atrial myocytes under shear stress (Fig. 9), consistent with the Ca^{2+} imaging results. Autocrine activation of P2X receptors via shear-induced connexin hemichannel activation may be an important mechanism by which atrial cells measure mechanical stimulus and translate it into altered excitability.

Shear-induced APs were preceded by a slow graded depolarization and their duration was significantly prolonged (Fig. 3A). Our data on the inhibition of T-wave initiation by P2X receptor antagonists suggest a possible role of P2X receptors in graded depolarization. P2X receptors are ionotropic receptors that permeate cations non-selectively [41], allowing cation influx at negative potentials. Under normal extracellular Ca^{2+} concentrations, most of the ATP-induced inward current is carried by Na^+, with Ca^{2+} contributing <10% of the total P2X inward current induced by ATP [42]. It has been shown in mouse ventricular myocytes that the increased Na^+ entry through the P2X receptors can enhance Ca^{2+} entry via the NCX [43]. In this regard, we have not consistently observed increases in background Ca^{2+} levels and/or in spontaneous Ca^{2+} spark occurrence prior to generation of T-wave under shear exposure (Fig. 2A–D, 5E and 6E), although some cells showed these phenomena (Fig. 1A, 5B, 6B and 7C). In addition, the preceding background Ca^{2+} changes were not correlated with frequency of T-waves and their latencies (data not shown). It should be also noted that we have not considered T-waves, occasionally starting from longitudinal Ca^{2+} wave in the present study. These waves, in fact, involve $P2Y_1$ receptor signaling, as has been previously reported [12]. Other regulatory mechanism activated by shear stress in cardiac myocytes, such as mitochondrial ROS-dependent RyR sensitization [14], may be involved in increases in background Ca^{2+} and resting Ca^{2+} sparks in atrial cells under shear stress, although this needs further confirmation.

We used freshly isolated atrial myocytes from rats to measure ATP release under shear stress. Our study is the first to show shear-induced ATP release in cardiac myocytes. The quantity of released ATP for 10-s-long shear exposure ($11x10^{-18}$ moles/μm^2) was comparable to the values measured in other cell types during mechanical stresses using a similar way of measurement [44]. Shear stress-induced ATP release has been demonstrated in vascular endothelial cells [16].]It has also been shown, in neonatal rat cardiac myocyte culture [31] and in HL-1 atrial cell line [21], that mechanical stretch causes ATP release. Interestingly, stretch-induced ATP release in those cardiac cells is known to be mediated by pannexins [21, 31]. This is in sharp contrast with our observations in rat atrial myocytes under shear stress that ATP release was probenecid-insensitive (Fig. 9G). In addition, ATP release by atrial myocyte under shear stress was distinctly enhanced by removal of external Ca^{2+} (Fig. 9D), which supports a role of connexins, but not pannexins, on the shear response.

The time-dependent decay of extracellular ATP concentration under shear stress appears to be similar to that observed under stretch in neonatal and HL-1 cardiac cells [21, 31]. All of these studies have used chemiluminescence measurements from cell-free external solutions using luciferin-luciferase assay. However, the time course of ATP release was distinct from time-independent T-wave propensity during the 10-20-s shear exposure. The luciferin-luciferase assay may only provide a rough estimation of the bulk concentration of ATP released from cells. In fact, the local ATP concentration in the vicinity of the cell surface is often found to be much higher and discordant from the bulk estimates [45, 46] due to delayed diffusion of ATP, unstirred layer effects and rapid degradation by cell surface ecto-ATPases.

In this study, we generally applied shear stress of ~16 dyn/cm^2 to single atrial cells. ATP release from atrial myocytes reached to maximum value at shear strength of ~8 dyn/cm^2. This shear strength is within the range (0.2–30 dyn/cm^2) of biologically effective shear forces in single cells [9-13, 23]. The shear strength is much higher than the interlaminar shear stress (0.4 dyn/cm^2) estimated in intact rat atrial tissue under physiological conditions [11]. We applied high shear stress to mimic the high intra-atrial fluid pressure under conditions of heart failure and valvular heart diseases. It may be difficult to estimate the shear force on single myocytes *in vivo* under pathological conditions. In addition, the shear force may differ significantly depending on disease status and between right and left hearts. In fact, in chronic mitral regurgitation, the endocardial surface is widely disrupted [7, 8], and atrial myocytes are directly subjected to higher shear stress. The clinical consequences of such regurgitation or volume overload are atrial fibrillation (AF) and remodeling [1, 5, 6]. We found evidence that atrial myocytes elicit AP-induced Ca^{2+} waves under shear stress, and that

P2X receptor activation by ATP efflux through connexin hemichannels may be responsible for such wave generation. Our data suggest that initial T-wave event during shear exposure may not be necessarily related to NCX, but that secondary T-wave generation may be facilitated by altered NCX activity via preceding depolarization/Ca^{2+} signalling. Shear-dependent pacemaker activity in atrial myocyte and prolonged depolarization with longer Ca^{2+} increase may, in part, contribute to atrial arrhythmogenesis. The pathophysiological implication of shear-induced T-waves needs further investigation.

Acknowledgements

The work was supported by National Research Foundation of Korea (NRF) grant funded by the Korean Government (MEST) (2017R1E1A1A01074504 and 2017K2A9A1A06056330).

Disclosure Statement

The authors declare no conflicts of interest.

References

1 Nazir SA, Lab MJ: Mechanoelectric feedback and atrial arrhythmias. Cardiovasc Res 1996;32:52–61.
2 Lakatta EG: Cardiovascular regulatory mechanisms in advanced age. Physiol Rev 1993;73:413–467.
3 LeGrice IJ, Takayama Y, Covell JW: Transverse shear along myocardiac cleavage planes provides a mechanism for normal systolic wall thickening. Circ Res 1995;77:182–193.
4 Costa KD, Takayama Y, McCuloch AD, Covell JW: Laminar fiber architecture and three-dimensional systolic mechanics in canine ventricular myocardium. Am J Physiol 1999;276:H595–H607.
5 Nattel S: New ideas about atrial fibrillation 50 years on. Nature 2002;415:219–226.
6 Schotten U, Verheule S, Kirchhof P, Goette A: Pathophysiological mechanisms of atrial fibrillation: a translational appraisal. Physiol Rev 2011;91(1):265–325.
7 Goldsmith I, Kumar P, Carter P, Blann AD, Patel RL, Lip GYH: Atrial endocardial changes in mitral valve disease: a scanning electron microscopy study. Am Heart J 2000;140:777–784.
8 Saffitz JE: Acquired valvular and endocardial diseases; in Rubin E & Reisner HM (ed): Essentials of Rubin's Pathology. 5th edn. Lippincott Williams & Wilkins, Inc. 2009, pp. 232–237.
9 Woo SH, Risius T, Morad M: Modulation of local Ca^{2+} release sites by rapid fluid puffing in rat atrial myocytes. Cell Calcium 2007;41:397–403.
10 Belmonte S, Morad M: 'Pressure-flow'-triggered intracellular Ca^{2+} transients in rat cardiac myocytes: possible mechanisms and role of mitochondria. J Physiol 2008;586.5:1379–1397.
11 Boycott HE, Barbier CSM, Eichel CA, Costa KD, Martins RP, Louault F, Dilanian G, Coulombe A, Hatem SN, Balse E: Shear stress triggers insertion of voltage-gated potassium channels from intracellular compartments in atrial myocytes. Proc Natl Acad Sci USA 2013;110(41):E3955–E3964.
12 Kim JC, Woo SH: Shear stress induces a longitudinal Ca^{2+} wave via autocrine activation of $P2Y_1$ purinergic signaling in rat atrial myocytes. J Physiol 2015;593:5091–5109.
13 Son MJ, Kim JC, Kim SW, Chidipi B, Muniyandi J, Singh TD, So I, Subedi KP, Woo SH: Shear stress activates monovalent cation channel transient receptor potential melastatin subfamily 4 in rat atrial myocytes via type 2 inositol 1, 4,5-trisphosphate receptors and Ca^{2+} release. J Physiol 2016;594:2985–3004.
14 Kim JC, Son MJ, Wang J, Woo SH: Regulation of cardiac Ca^{2+} and ion channels by shear mechanotransduction. Arch Pharm Res 2017;40(7):783–795.
15 Vassort G: Adenosine 5'-trisphosphate: a P2-purinergic agonist in the myocardium. Physiol Rev 2001;81:767–806.
16 Yamamoto K, Sokabe T, Ohura N, Nakatsuka H, Kamiya A, Ando J: Endogenously released ATP mediates shear stress-induced Ca^{2+} influx into pulmonary artery endothelial cells. Am J Physiol Heart Circ Physiol 2003;285:H793–H803.

17 Sabirov RZ, Okada Y: Wide nanoscopic pore of maxi-anion channel suits its function as an ATP-conductive pathway. Biophys J 2004;87:1672-1685.
18 Bell PD, Kobatake E, Aizawa M, Dubyak GR: Detection of local ATP release from activated platelets using cell surface-attached firefly luciferase. Am J Physiol 2003;276:C267–C278.
19 Schneider SW, Egan ME, Jena BP, Guggino WB, Oberleithner GH, Geibel JP: Continuous detection of extracellular ATP on living cells by using atomic force microscopy. Proc Natl Acad Sci USA 1999;96:12180–12185.
20 Stout CE, Costantin JL, Naus CC, Charles AC: Intercellular calcium signaling in astrocytes via ATP signaling in astrocytes. Anal Chem 2000;72:10482–10488.
21 Oishi S, Sasano T, Tateishi Y, Tamura N, Isobe M, Furukawa T: Stretch of atrial myocytes stimulates recruitment of macrophages via ATP released through gap-junction channels. J Pharmacol Sci 2012;120:296–304.
22 Bodin P, Burnstock G: Evidence that release of adenosine trisphosphate from endothelial cells during increased shear stress is vesicular. J Cardiovasc Pharmacol 2001;38:900–908.
23 Olesen SP, Clapham DE, Davies PF: Hemodynamic shear stress activates a K^+ current in vascular endothelial cells. Nature 1988;331:168–170.
24 Woo SH, Cleemann L, Morad M: Ca^{2+}-current-gated focal and local Ca^{2+} release in rat atrial myocytes: evidence from rapid 2-D confocal imaging. J Physiol 2002;543:439–453.
25 Hüser J, Lipsius SL, Blatter LA: Calcium gradients during excitation-contraction coupling in atrial myocytes. J Physiol 1996;494:641–651.
26 Kockskämper J, Sheehan KA, Bare DJ, Lipsius SL, Mignery GA, Blatter LA: Activation and propagation of Ca^{2+} release during excitation-contraction coupling in atrial myocytes. Biophys J 2001;81(5):2590–2605.
27 Mackenzie, L. Bootman MD, Berridge MJ, Lipp P: Predetermined recruitment of calcium release sites underlies excitation-contraction coupling in rat atrial myocytes. J Physiol 2001;530:417–429.
28 Forssmann WG, Girardier L: A study of the T system in rat heart. J Cell Biol 1970;44:1–19.
29 Fill M, Copello J: Ryanodine receptor calcium release channels. Physiol Rev 2002;82:893–922.
30 Musa H, Tellez JO, Chandler NJ, Greener ID, Maczewski M, Mackiewicz U, Beresewicz A, Molenaar P, Boyett MR, Dobrzynski H: P2 purinergic receptor mRNA in rat and human sinoatrial node and other heart regions. Naunyn Schmiedebergs Arch Pharmacol 2009;379 (6):541–549.
31 Nishida M, Sato Y, Uemura A, Narita Y, Tozaki-Saitoh H, Nakaya M, Ide T, Suzuki K, Inoue K, Nagao T, Kurose H: P2Y6 receptor-Gα12/13 signaling in cardiomyocytes triggers pressure overload-induced cardiac fibrosis. EMBO J 2008;27:3104–3115.
32 Kienitz MC, Bender K, Dermietzel R, Pott L, Zoidl G: Pannexin 1 constitutes the large conductance cation channel of cardiac myocytes. J Biol Chem 2011;286:290–298.
33 Silverman W, Locovei S, Dahl G: Probenecid, a gout remedy, inhibits pannexin 1 channels. Am J Physiol Cell Physiol 2008;295:C761–C767.
34 Connolly GP: Differentiation by pyridoxal 5-phosphate, PPADS and IsoPPADS between responses mediated by UTP and those evoked by alpha, beta-methylene-ATP on rat sympathetic ganglia. Br J Pharmacol 1995;114(3):727–731.
35 Lewis CJ, Evans RJ: Comparison of P2X receptors in rat mesenteric, basilar and septal (coronary) arteries. J Auton Nerv Syst 2000;81:69–74.
36 Prosser BL, Ward CW, Lederer WJ: X-ROS signaling: Rapid mechano-chemo transduction in heart. Science 2011;333:1440–1445.
37 Jian Z, Han H, Zhang T, Puglisi J, Izu LT, Shaw JA, Onofiok E, Erickson JR, Chen YJ, Horvath B, Shimkunas R, Xiao W, Li Y, Pan T, Chan J, Banyasz T, Tardiff JC, Chiamvimonvat N, Bers DM, Lam KS, Chen-Izu Y: Mechanochemotransduction during cardiomyocyte contraction is mediated by localized nitric oxide signaling. Sci Signal 2014;7 (317):ra27.
38 Simard C, Sallé L, Rouet R, Guinamard R: Transient receptor potential melastatin 4 inhibitor 9-phenanthrol abolishes arrhythmias induced by hypoxia and re-oxygenation in mouse ventricle. Br J Pharmacol 2012;165:2354–2364.
39 Song Y, Shryock JC, Belardinelli L: An increase of late sodium current induces delayed afterdepolarizations and sustained triggered activity in atrial myocytes. Am J Physiol Heart Circ Physiol 2008;294:H2031–H2039.

40 John SA, Kondo R, Yang SY, Goldhaber JI, Weiss JN: Connexin-43 hemichannels opened by metabolic inhibition. J Biol Chem 1999;274:236–240.
41 North RA: Molecular physiology of P2X receptors. Physiol Rev 2002;82:1013–1067.
42 Garcia-Guzman M, Soto F, Gomez-Hernandez JM, Lund PE, Stuhmer W: Characterization of recombinant human P2X4 receptor reveals pharmacological differences to the rat homologue. Mol Pharmacol 1997;51:109–118.
43 Shen JB, Yang R, Pappano A, Liang BT: Cardiac P2X purinergic receptors as a new pathway for increasing Na^+ entry in cardiac myocytes. Am J Physiol Heart Circ Physiol 2014;307:H1469–H1477.
44 McLatchie LM, Fry CH: ATP release from freshly isolated guinea-pig bladder urothelial cells: a quantification and study of the mechanisms involved. BJU Int 2015;115:987–993.
45 Yamamoto K, Furuya K, Nakamura M, Kobakake E, Sokabe M, Ando J: Visualization of flow-induced ATP release and triggering of Ca^{2+} waves at caveolae in vascular endothelial cells. J Cell Sci 2011;124:3477–3483.
46 Proost ID, Pintelon I, Wilkinson WJ, Goethals S, Brouns I, Nassauw LV, Riccardi D, Timmermans JP, Kemp PJ, Adriaensen D: Purinergic signaling in the pulmonary neuroepithelial body microenvironment unraveled by live cell imaging. FASEB J 2009;23:1153–1160.